A MODEL FOR BISTATIC SCATTERING FROM TRAPPED GAS BUBBLES IN SANDY SEDIMENTS

F A Boyle (1) & N P Chotiros (1)

(1) Applied Research Laboratories, The University of Texas at Austin, Austin, TX

1. INTRODUCTION

The literature contains a variety of models for acoustic backscatter from marine sediments. They are based on several different hypothetical mechanisms. Some models, like those of Patterson[1], and Clay and Medwin[2] are based on roughness scattering from the water-sediment interface. Others, including those of Nolle et.al.[3], Stockhausen[4], Ivakin et.al.[5], and Jackson et.al.[6] include scattering from within the sediment volume below the interface. The volume scattering mechanisms usually involve scattering from grains or fluid pockets or inhomogeneities in the refractive index of the sediment, caused by variations in soundspeed or density. The subject of this paper is a new hypothetical mechanism: resonance scattering from trapped bubbles.

In 1990, Chotiros et.al.[7] performed a comprehensive compilation of shallow grazing angle backscatter measurements. The data were collected from all published sources worldwide and included measurements from the 1950's to the present. Figure 1 is an illustration of Chotiros' compilation. Here, backscattering strength measurements are plotted against normalized grain size, which is defined as the grain diameter divided by the acoustic wavelength. The data span a region bounded in the upper limit by Lambert's rule and in the lower limit by the results of Nolle's experiments[8] over degassed laboratory sands. A distinguishing feature of Nolle's data is that the backscattering strength increases steadily with normalized grain size.

In Fig. 2, data points from a common site are connected with lines; two trends emerge. In group 1, the backscattering strength increases monotonically with normalized grain size, just like Nolle's data over degassed sands. In group 2, there is a broad maximum in the backscattering strength when the grain diameter is $10^{-2.5}$ wavelengths. The fact that this is close to the resonance diameter of gas bubbles in water suggests a hypothesis: a dominant mechanism for acoustic scattering in marine sands might involve resonance scattering from bubbles trapped within the sediment. In order to investigate this hypothesis, a volume scattering model was developed, based on resonance scattering from a spatial distribution of gas bubbles in the sediment.

In section 2, the acoustic penetration and propagation model is described. Section 3 contains a description of the trapped bubble backscatter mechanism. In section 4, the resulting expression for acoustic backscattering strength is developed. Bistatic scattering is then discussed in section 5. Comparisons of the model with experiment follow in section 6. A discussion of the results is contained in section 7.

A MODEL FOR BISTATIC SCATTERING FROM TRAPPED GAS BUBBLES IN SANDY SEDIMENTS

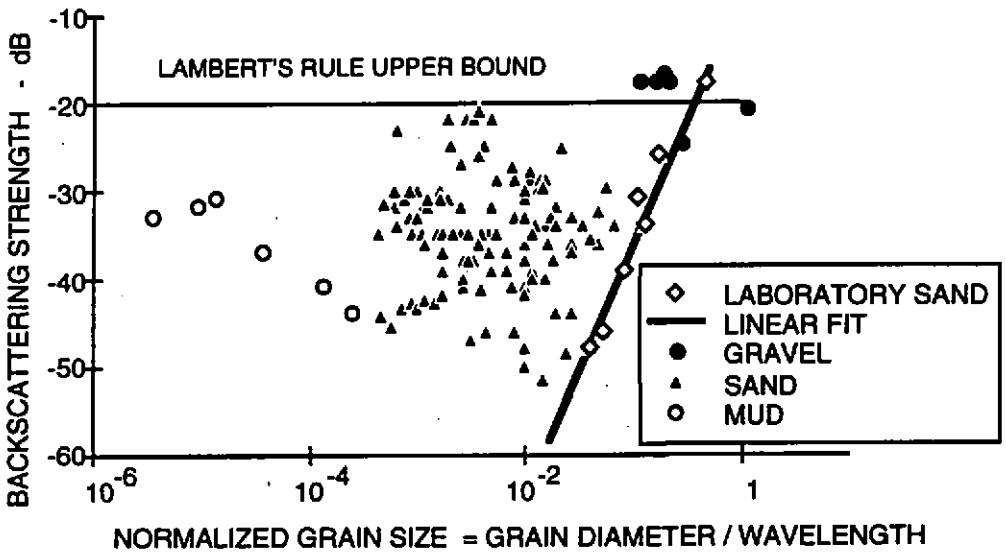

Figure 1. Experimental measurements of bottom backscattering strength as a function of grain size at a grazing angle of 10° from all published sources.

A MODEL FOR BISTATIC SCATTERING FROM TRAPPED GAS BUBBLES IN SANDY SEDIMENTS

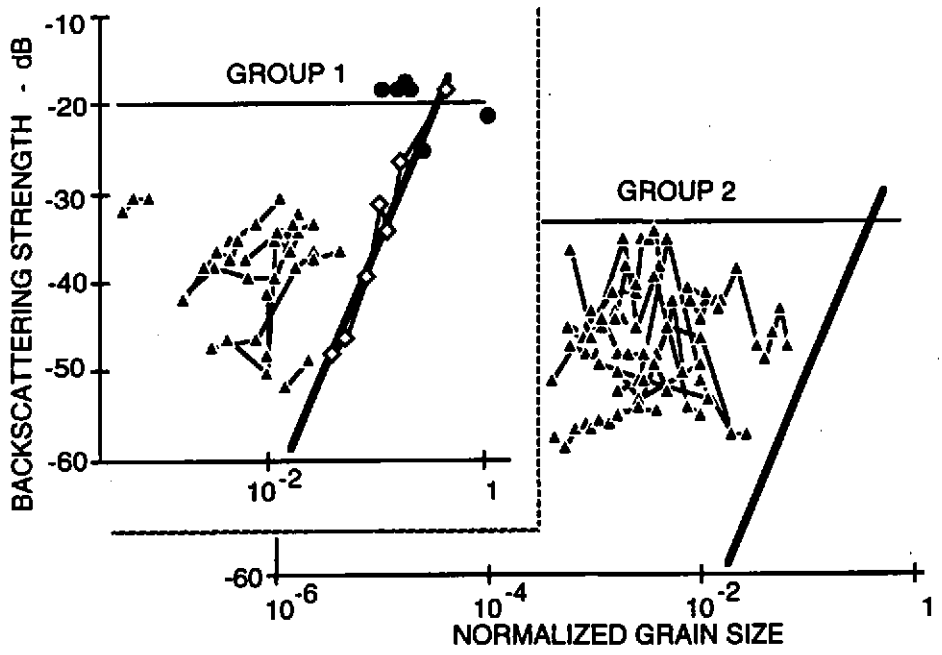

Figure 2. Experimental measurements of bottom backscattering strength as a function of grain size at a grazing angle of 10°, groups 1 & 2.

A MODEL FOR BISTATIC SCATTERING FROM TRAPPED GAS BUBBLES IN SANDY SEDIMENTS

2. BIOT MODEL FOR ACOUSTIC PROPAGATION

Recent experiments[9,10] suggest that acoustic propagation in sandy sediments can be modeled with the Biot theory[11,12]. The Biot theory, unlike other common sediment models, treats the sediment as a two phase medium. The sand grains form a solid skeletal frame through which a fluid phase is allowed to flow. Biot derived the following coupled pair of differential equations of motion for the system:

$$N\nabla^2\mathbf{u} + \text{grad}[(A+N)e + Q\varepsilon] = \frac{\partial^2}{\partial t^2}(\rho_{11}\mathbf{u}+\rho_{12}\mathbf{U}) + b\frac{\partial}{\partial t}(\mathbf{u}-\mathbf{U}) \quad , \tag{1}$$

$$\text{grad}[Qe + R\varepsilon] = \frac{\partial^2}{\partial t^2}(\rho_{12}\mathbf{u}+\rho_{22}\mathbf{U}) - b\frac{\partial}{\partial t}(\mathbf{u}-\mathbf{U}) \tag{2}$$

where

$\mathbf{u}$ = solid displacement vector
$\mathbf{U}$ = Fluid displacement vector
e = div $\mathbf{u}$
ε = div $\mathbf{U}$
N,A,Q,R,b=constants
ρ_{11},ρ_{12},ρ_{22}=constants involving densities
$\rho_{11}+\rho_{12}$=mass of solid per unit volume of aggregate
$\rho_{12}+\rho_{22}$=mass of fluid per unit volume of aggregate
ρ_{12}=coupling coefficient.

An interesting feature of this pair of equations is that there are two compressional wave solutions. The Biot fast wave corresponds to a mode wherein the fluid and solid parts move roughly in phase. This is analogous to the "P" wave supported by an ordinary elastic medium. The Biot slow wave has the fluid and solid parts moving roughly out of phase.

Because of the relative motion between fluid and solid, slow waves are expected to attenuate rapidly due to viscous and inertial losses, leaving the fast wave to dominate. In this case, it is appropriate to neglect the slow waves altogether. Single phase models of the sediment are therefore often adequate in acoustic modeling of the sea floor.

Recent experiments however suggest that under some conditions, specifically shallow grazing angles and high frequencies, slow waves cannot be neglected. Since the speed of the fast wave is generally greater than that of the acoustic wave in the water column above, there exists a critical grazing angle, below which Biot fast waves in the sediment will totally reflect back up into the water column above. An evanescent wave will be generated, with a penetration depth that is shallow at high frequencies. Since slow waves have a phase velocity less than that of the water column, they refract downward. There is therefore no critical angle for Biot slow waves, which are left to dominate at shallow grazing angles and high frequencies.

The Biot theory incorporated into this model is that of Stern, Bedford, and Millwater[13]. Given a plane wave source in the water column, it predicts pore fluid velocities and pressures at any depth in the sediment column.

3. SCATTERING CROSS SECTION OF A SEDIMENT VOLUME ELEMENT

The assumed scattering mechanism in this model is resonance scattering from trapped bubbles in the sediment matrix. The resulting expression for the volume scattering cross section σ_{bv} of an element of sediment volume is

$$\sigma_{bv} = \int_0^\infty N(r_b)\, \sigma(r_b)\, dr_b \ , \qquad (3)$$

where r_b is the bubble radius and $\sigma(r_b)$ is the scattering cross section of a single bubble. The bubble size distribution function $N(r_b)$ is defined as the number of bubbles per unit volume per unit radius increment.

In writing Eq. (3), it is assumed that multiple scattering between bubbles is negligible. The justification of this assumption arises from the narrow resonance band of the scattering bubbles. Any two bubbles that couple must have very close to the same resonance frequency. In a broad distribution of bubble sizes, neighboring mutual scatterers must be widely spaced. A detailed discussion of the justification for the single scatter assumption has been submitted by the authors for publication[14].

In order to solve Eq. (3), $N(r_b)$ and $\sigma(r_b)$ must be determined. An estimate for $N(r_b)$ is described in subsection A. Subsection B contains an expression for $\sigma(r_b)$. In subsection C the resulting expression for σ_{bv} is presented.

3.1 Bubble Size Distribution Function $N(r_b)$

The authors are not aware of any direct measurements of trapped bubble size distributions in sandy sediments. An estimate is constructed, based on the grain size distribution, which can be measured. Since grain size distributions are approximately log-normal, it is convenient to express the bubble size distributions in terms of $z = \ln(r_b)$.

The estimate is based on the assumption that a trapped bubble's size is governed by the size of the surrounding sediment pore. The bubble size distribution N(z) therefore has the same shape as the pore size distribution $f_p(z)$:

$$N(z) = \xi\, f_p(z - \ln(r_{bp})) \ , \qquad (4)$$

where r_{bp} is the ratio of bubble radius to surrounding pore radius and ξ is the fraction of pores that contain a bubble.

There are no direct measurements of the pore size distribution function f_p in sandy sediments. Such distributions have, however, been measured for dense random packings of hard spheres[15,16].

Figure 3 is a plot of the pore size distribution in such a medium. The fact that the porosities of these dense random packings coincide with measured porosities of sandy sediments suggests a similar packing structure. If the assumption is made that sands pack like dense random packings of hard spheres, an estimate of the sandy sediment pore size distribution can be constructed by convolving the grain size distribution with the pore size distribution of a dense random packing:

$$f_p(y) = f_x(x) * p(x,y) \quad , \tag{5}$$

where

x = in (grain radius),
y = in (pore radius),
$f_x(x)$ = grain radius distribution function,
$p(x,y)$ = pore radius distribution function in a dense random packing of hard spheres with radius x.

3.2 Scattering Cross Section of a Single Bubble

An expression for the scattering cross section of a single bubble of radius r_b is given by Wildt[17]:

$$\sigma(r_b) = \frac{4\pi r_b^2}{\left[\left(\frac{f_r}{f}\right)^2 - 1\right]^2 + \delta^2} \quad , \tag{6}$$

where f is the acoustic frequency. The resonance frequency f_r, and the damping constant δ are both functions of the bubble radius r_b. If Eq. (6) is substituted into Eq. (3), the resulting integral is difficult to solve analytically. In order to facilitate this integral, the approximation for the bubble scattering cross section developed by Medwin[18] is used:

$$\sigma(r_b) \approx 2\pi^2\left(\frac{a_r^3}{\delta}\right)\delta_{a_r}(r_b) \quad , \tag{7}$$

where $\delta_{ar}(r_b)$ is a Dirac delta function of the bubble radius about the resonance radius a_r, which is given by

$$a_r = \frac{\sqrt{\frac{3\gamma b\beta P_0}{\rho}}}{2\pi f} \quad , \tag{8}$$

where γ is the ratio of specific heats c_p/p_v for the gas inside the bubble, b and β are constants involving surface tension and thermal conductivity, P_0 is the ambient pressure, and ρ is the water density.

A MODEL FOR BISTATIC SCATTERING FROM TRAPPED GAS BUBBLES IN SANDY SEDIMENTS

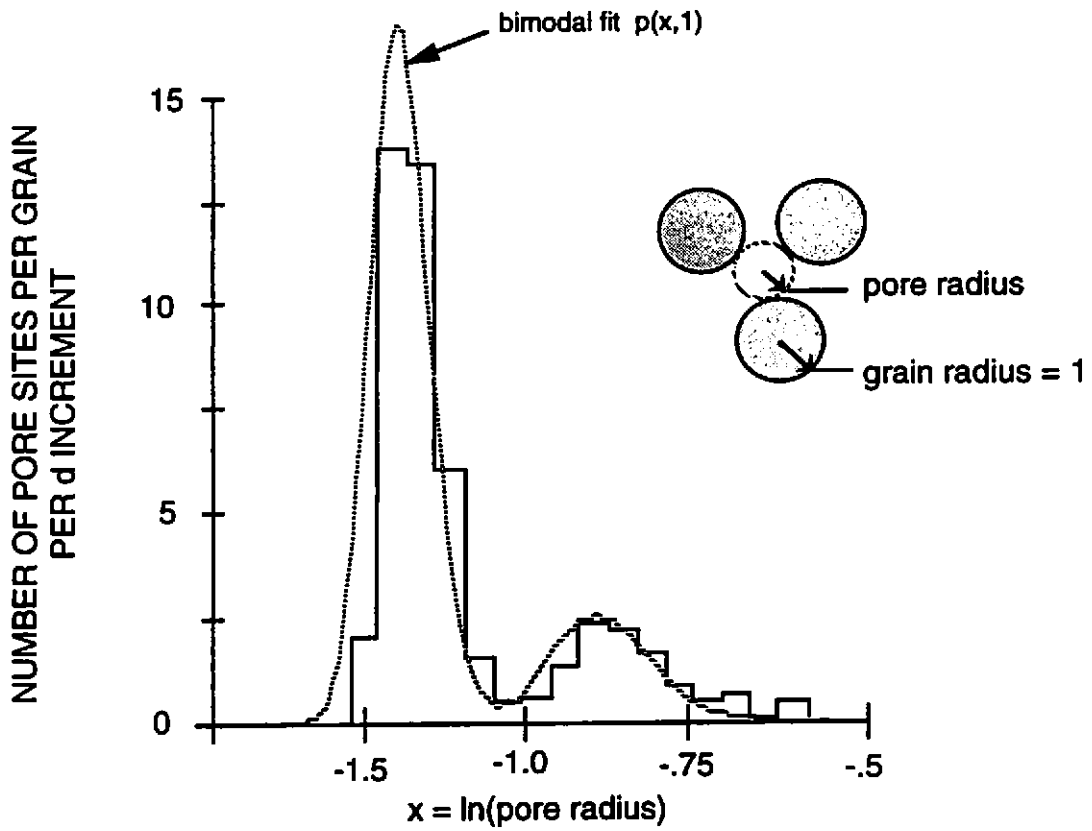

Figure 3. Distribution of interstitial pore sizes for dense random packing of spherical grains of unit radius.

A MODEL FOR BISTATIC SCATTERING FROM TRAPPED GAS BUBBLES IN SANDY SEDIMENTS

3.3 Sediment Volume Scattering Cross Section

By inserting Eq. (7) into Eq. (3), a simple form for the sediment scattering cross section per unit volume is obtained:

$$\sigma_{bv} = N(a_r)\, 2\pi^2 \left(\frac{a_r^3}{\delta}\right) , \tag{9}$$

where a_r is given by Eq. (8).

4. BACKSCATTERING STRENGTH OF THE WATER/SEDIMENT INTERFACE

The backscatter from a sediment interface element can be defined as the sum of contributions from all volume elements below the interface. In subsection A, the backscattered pressure contribution from an element of sediment volume is developed. In subsection B, the contributions from volume elements below the interface are summed to get an effective interface backscattering strength.

4.1 Backscatter contribution from an element of sediment volume by reciprocity

Figure 4 illustrates the method used to obtain the backscatter contribution from an element dxdydz of sediment volume. First, virtual spheres with radius r much greater than the acoustic wavelength λ are drawn around projector and scattering element.

The virtual sphere surrounding the projector has a surface velocity v_0, which induces a pressure p_1 at the location of the scatterer. The scatterer responds with a scattered surface velocity v_1', which produces a backscattered pressure p_2 at the source. These pressures and surface velocities can be related by the principle of acoustic reciprocity, which states that, in a linear medium, a source and receiver can be swapped with no change in the ratio of received to transmitted signals. This swapping of positions can be interpreted to represent the backscatter case, where the scatterer acts as a projector and the source as a receiver. In the context of the present backscatter problem, the reciprocity principle states:

$$\frac{p_1}{v_0} = \frac{p_2}{v_1'} . \tag{10}$$

The surface velocities v_0 and v_1' of the virtual spheres can be related to local pressures and acoustic impedances:

$$v_0 = \frac{p_0}{Z_0} , \tag{11}$$

$$v_1' = \frac{\varepsilon p_1}{Z_1} , \tag{12}$$

where p_0, v_0, and Z_0 are the acoustic pressure, fluid velocity, and acoustic impedance at the surface of the virtual sphere surrounding the projector. v_1' and Z_1 are the fluid velocity and impedance at the

A MODEL FOR BISTATIC SCATTERING FROM TRAPPED GAS BUBBLES IN SANDY SEDIMENTS

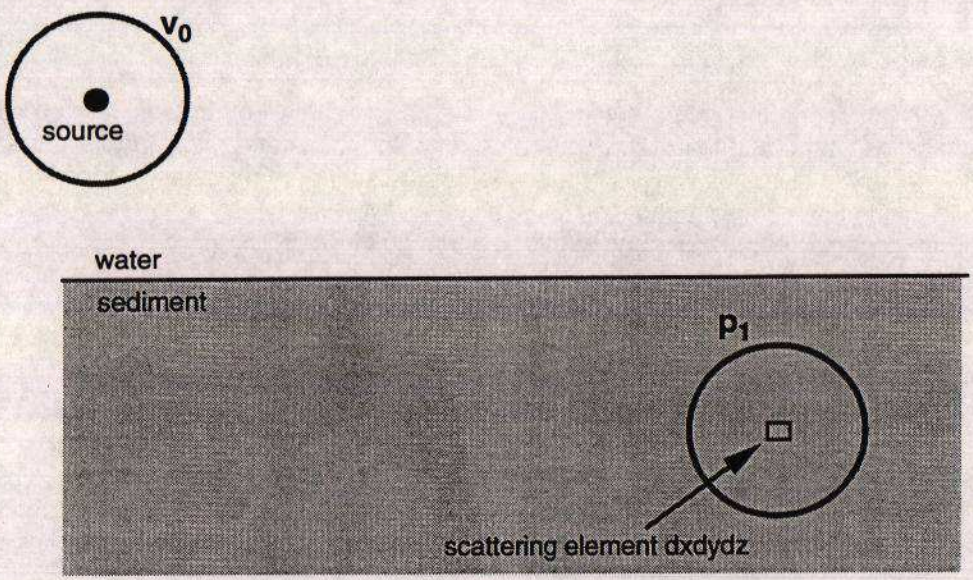

a. acoustic propagation of incident sound

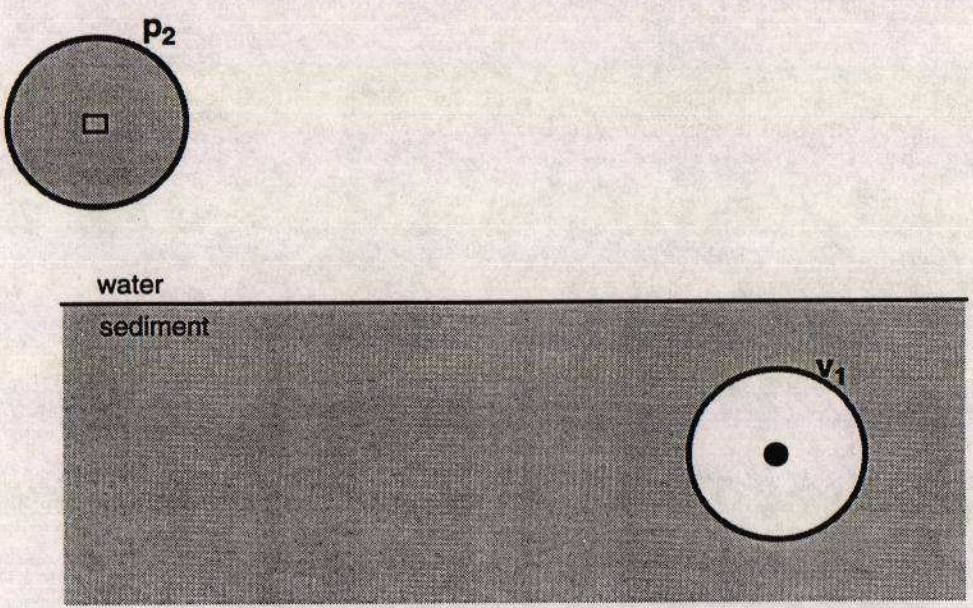

b. acoustic propagation of backscattered sound

Figure 4. Reciprocity as applied to virtual spheres of equal radius about source and scatterer. The radius is much greater than the acoustic wavelength so that plane wave acoustic impedances can be used, and much smaller than the separation between source and scatterer so that the projected pressure amplitudes $|p_1|$ and $|p_2|$ are approximately constant across the spheres' surfaces.

sphere surrounding the scattering volume element. ε is a transfer function from incident pressure $\mathbf{p_1}$ to scattered pressure $\varepsilon\mathbf{p_1}$ at the surface of the sphere surrounding the scatterer. It includes the effects of scattering at the element dxdydz, as well as propagation of the scattered pressure to the virtual sphere's surface. As illustrated in Fig. 4, this propagation takes place as if it were in the water column. If attenuation in the water column is neglected, the average square magnitude of ε is

$$\langle|\varepsilon|^2\rangle = \frac{\sigma_{bv}\,dxdydz}{4\pi r_s^2} \quad , \tag{13}$$

where dxdydz is the sediment volume element and r_s is the radius of the virtual spheres surrounding source and scatterer. σ_{bv} is the volume scattering cross section, defined as ratio of scattered power to incident intensity for the sediment volume scattering element, averaged over the complete ensemble of possible bubble distributions within dxdydz. Equations (10), (11), (12), and (13) can be combined to obtain an expression for the square magnitude of the acoustic pressure returned to the projector:

$$\langle|\mathbf{p_2}|^2\rangle = \int \left|\frac{\mathbf{p_1}}{\mathbf{p_0}}\right|^2 \frac{\sigma_{bv}}{4\pi r_s^2} \left|\frac{\mathbf{Z_0}}{\mathbf{Z_1}}\mathbf{p_1}\right|^2 dxdydz \quad . \tag{14}$$

Since the radius of the virtual spheres was assumed large in comparison to the wavelength λ, plane wave acoustic impedances[19] can be used for $\mathbf{Z_0}$ and $\mathbf{Z_1}$:

$$|\mathbf{Z_0}| = \left|\frac{\mathbf{p_0}}{\mathbf{v_0}}\right| = \rho_0 c_0 \quad , \tag{15}$$

$$|\mathbf{Z_1}| = \left|\frac{\mathbf{p_1}}{\mathbf{v_1}}\right| = \rho_1 c_1 \quad , \tag{16}$$

where $\mathbf{p_0}$, $\mathbf{v_0}$, $\mathbf{p_1}$, and $\mathbf{v_1}$ are plane wave acoustic pressures and fluid velocities in the water column and sediment, respectively. ρ_0 and ρ_1 are water and sediment densities and c_0 and c_1 are corresponding phase velocities.

If the Biot theory is used to calculate sediment acoustic pressures, the simultaneous presence of Biot fast and slow acoustic waves will affect the form of the returned pressure amplitude, Eq.(14):

$$\langle|\mathbf{p_2}|^2\rangle = \int \left|\frac{\mathbf{p_1}}{\mathbf{p_0}}\right|^2 \left(\frac{\sigma_{bvf}}{4\pi r_s^2} \left|\frac{\mathbf{Z_0}}{\mathbf{Z_{1f}}}\mathbf{p_{1f}}\right|^2 + \frac{\sigma_{bvs}}{4\pi r_s^2} \left|\frac{\mathbf{Z_0}}{\mathbf{Z_{1s}}}\mathbf{p_{1s}}\right|^2 \right) dxdydz \tag{17}$$

The two terms inside the parentheses are the separate effects of Biot fast and slow waves in the sediment. The pressures $\mathbf{p_{1f}}$ and $\mathbf{p_{1s}}$ are pore pressures carried by each wave. Similarly, there are separate acoustic impedances $\mathbf{Z_{1f}}$, $\mathbf{Z_{1s}}$ and scattering cross sections σ_{bvf}, σ_{bvs}.

A MODEL FOR BISTATIC SCATTERING FROM TRAPPED GAS BUBBLES IN SANDY SEDIMENTS

4.1 Sediment Interface Backscattering Strength

Figure 5 illustrates how the volume scattering from below a sediment interface can be recast as effective interface scattering. $\mathbf{p_{bs}}$ is the backscattered pressure from a sediment interface element. Its average square magnitude is the sum of contributions from all volume elements below the interface:

$$\langle |p_{bs}|^2 \rangle = \int_0^{-\infty} \left|\frac{p_1}{p_0}\right|^2 \left(\frac{\sigma_{bvf}}{4\pi r_s^2} \left|\frac{Z_0}{Z_{1f}} p_{1f}\right|^2 + \frac{\sigma_{bvs}}{4\pi r_s^2} \left|\frac{Z_0}{Z_{1s}} p_{1s}\right|^2 \right) dz \quad . \tag{18}$$

As illustrated in Fig. 6, the backscattering strength of a sediment interface element can be defined in terms of the pressure $\mathbf{p_{inc}}$ incident upon the interface and the scattered pressure $\mathbf{p_s}$ at unit distance from the element:

$$BS = 10 \log \frac{\langle |p_s|^2 \rangle}{|p_{inc}|^2} \quad . \tag{19}$$

These pressures can be related to the projected and backscattered pressures $\mathbf{p_0}$ and $\mathbf{p_{bs}}$ at the source,

$$|p_s| = |p_{bs}| \frac{r}{r_{1m}} e^{r\alpha} \quad , \tag{20}$$

$$|p_{inc}| = |p_0| \frac{r_s}{r} e^{-r\alpha} \quad , \tag{21}$$

where r is the separation between the projector and the interface element and r_{1m} is the unit radius. r_s is the radius of the virtual spheres surrounding source and scatterer. α is the absorption coefficient of the water column in units of Nepers per unit distance. By combining Equations (18), (19), (20), and (21) a simple expression for the backscattering strength is obtained:

$$BS = 10 \log \left(\frac{\left(\frac{1}{r_{1m}^2}\right) \int_0^{-\infty} |p_1|^2 \left(\frac{\sigma_{bvf}}{4\pi} \left|\frac{Z_0}{Z_{1f}} p_{1f}\right|^2 + \frac{\sigma_{bvs}}{4\pi} \left|\frac{Z_0}{Z_{1s}} p_{1s}\right|^2 \right)}{|p_{inc}|^4} \right) \quad . \tag{22}$$

5. BISTATIC SCATTERING STRENGTH

In Fig. 7, the bistatic scattering from an element of sediment volume is illustrated. A source at position A insonifies a sediment volume element at position B, which then scatters acoustic energy to a receiver at C. The scattered pressures at C can be computed by reciprocity in a similar manner as was done for the backscatter case.

A MODEL FOR BISTATIC SCATTERING FROM TRAPPED GAS BUBBLES IN SANDY SEDIMENTS

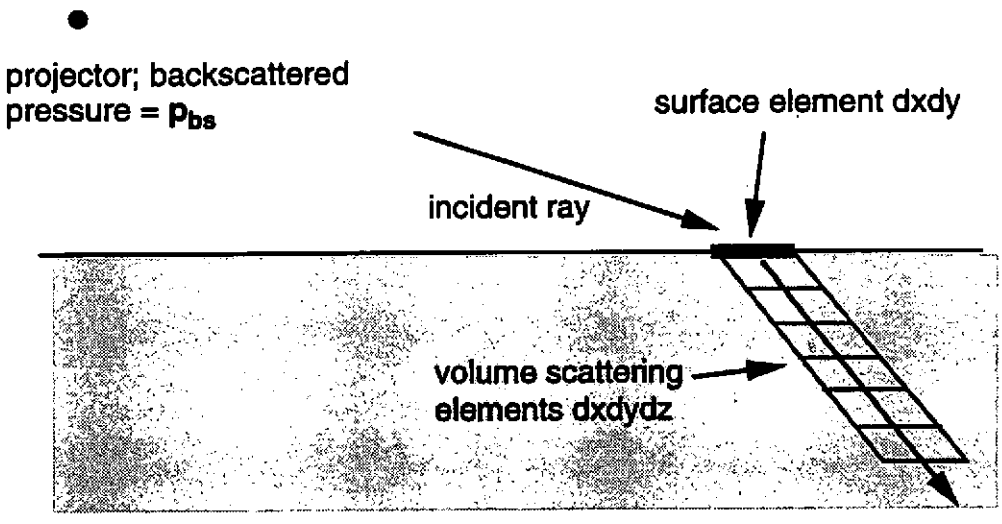

Figure 5: Backscatter from the volume below surface element dxdy.

A MODEL FOR BISTATIC SCATTERING FROM TRAPPED GAS BUBBLES IN SANDY SEDIMENTS

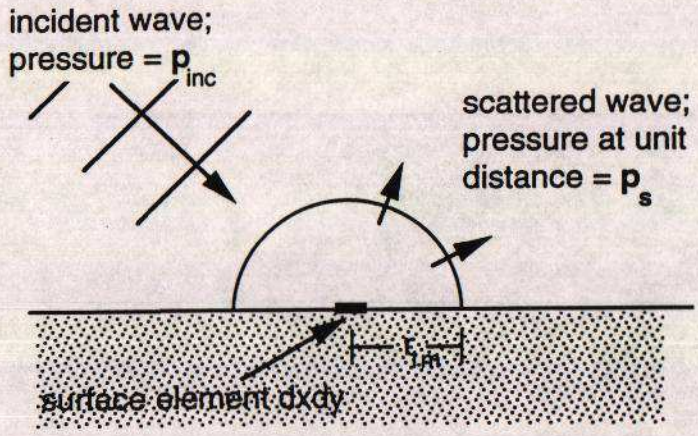

Figure 6: Backscatter from sediment interface element dxdy expressed in terms of incident and backscattered pressure.

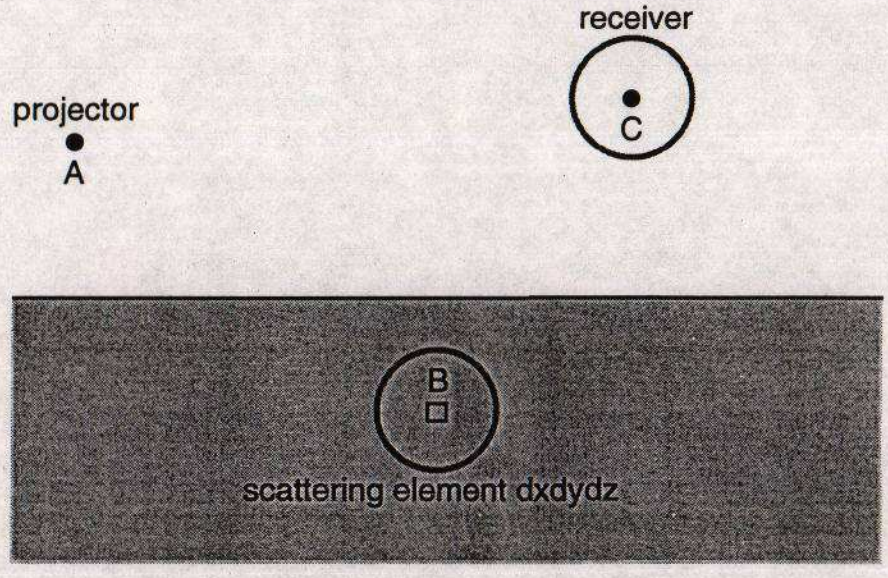

Figure 7. Calculation of bistatic scattering strength by reciprocity.

A MODEL FOR BISTATIC SCATTERING FROM TRAPPED GAS BUBBLES IN SANDY SEDIMENTS

The procedure is as follows. First, the scatterer at B and the receiver at C are surrounded by virtual spheres with radius $r_S >> \lambda$. The pressure at B that would be induced by a unit velocity at the surface of the virtual sphere at C can be computed by way of the Biot theory. By reciprocity, the pressure at C due to a unit velocity at the surface of B is the same. This pressure is then multiplied by the scattered surface velocity at B that is produced when B is insonified by the source at A. The square magnitude of pressure at the receiver due to bistatic scattering from a volume element dxdydz is given by

$$\langle |p_2|^2 \rangle = \int_0^{\infty} \left|\frac{p_b}{p_c}\right|^2 \left(\frac{\sigma_{bvf}}{4\pi r_s^2} \left|\frac{Z_0}{Z_{1f}} p_{1f}\right|^2 + \frac{\sigma_{bvs}}{4\pi r_s^2} \left|\frac{Z_0}{Z_{1s}} p_{1s}\right|^2 \right) dxdydz \quad , \tag{23}$$

where p_b is the total pore pressure at the scattering element that would be induced by a pressure p_c at the surface of the virtual sphere of radius r_S surrounding the receiver at C. Just as was done in Eq. (18) for the backscatter case, the square pressure from an interface element dxdy is defined as the sum of contributions from all volume elements below dxdy,

$$\langle |p_{fs}|^2 \rangle = \int_0^{\infty} \left|\frac{p_b}{p_c}\right|^2 \left(\frac{\sigma_{bvf}}{4\pi r_s^2} \left|\frac{Z_0}{Z_{1f}} p_{1f}\right|^2 + \frac{\sigma_{bvs}}{4\pi r_s^2} \left|\frac{Z_0}{Z_{1s}} p_{1s}\right|^2 \right) dz \quad . \tag{24}$$

The interface bistatic scattering strength defined in terms of the scattered and incident pressures at the interface:

$$SS = 10 \log \frac{\langle |p_s|^2 \rangle}{|p_{inc}|^2} \quad , \tag{25}$$

where the pressure p_s at unit distance from the interface is related to the pressure p_{fs} at the receiver at C:

$$|p_s| = |p_{fs}| \frac{r_c}{r_{1m}} e^{r_c \alpha} \quad , \tag{26}$$

where r_c is the distance from surface element dxdy to the receiver. The bistatic scattering strength of the interface is given by combination of Eqs. (24 - 26):

$$SS = 10 \log \left(\frac{\left(\frac{r_c}{r_{1m}}\right)^2 e^{2r_c\alpha} \int_0^{\infty} \left|\frac{p_b}{p_c r_s}\right|^2 \left(\frac{\sigma_{bvf}}{4\pi} \left|\frac{Z_0}{Z_{1f}} p_{1f}\right|^2 + \frac{\sigma_{bvs}}{4\pi} \left|\frac{Z_0}{Z_{1s}} p_{1s}\right|^2 \right) dz}{|p_{inc}|^2} \right) \tag{27}$$

A MODEL FOR BISTATIC SCATTERING FROM TRAPPED GAS BUBBLES IN SANDY SEDIMENTS

6. COMPARISONS WITH EXPERIMENT

The model requires specification of several input parameters, most of which can be estimated or measured. Two of the parameters, the gas fraction ζ and the bubble/pore size ratio r_{bp}, are unknown. These are treated as free parameters and are varied to fit the model to experimental data. Model input parameters for four of the group 2 backscatter sites are listed in Table 1. Figure 8 contains comparisons of the model with backscatter data from these sites. In each case, ζ and r_{bp} were adjusted to achieve a best fit of the model to data. The resulting gas fractions ζ varied between 1×10^{-6} and 1×10^{-5}. r_{bp}'s varied between 1.71 and 8.43.

The fact that the bubble/pore radius ratios r_{bp} were greater than 1 suggests that the assumed bubble size distributions are inaccurate. This may be a result of the assumption that bubble size distributions mirror those of the interstitial pores. Other factors, such as surface tension may have considerable influence on the bubble size distribution.

The behavior of the model matches observations well. The observed peak in backscattering strength is predicted by the model, given appropriate values for ζ and r_{bp}. In order to match the peak as it has been observed, very small gas fractions are sufficient. At present, the authors are aware of no practical way of measuring such small gas fractions in sediments.

7. DISCUSSION

A heuristic model for bistatic scattering from gas bubbles in sandy sediments has been developed. The model is consistent with a broad maximum in the observed backscattering strength at several sites, suggesting that bubble resonance may constitute a significant part of the scattering problem. The model can be fit to data by adjusting the gas fraction and the bubble/pore radius ratio as free parameters.

Very small gas fractions of 10^{-5} or less appear to be sufficient to produce observed backscatter for the sites that were observed. The authors are aware of no direct way of measuring gas fractions this small, so there is at present no independent verification for the model.

In order to allow an estimate of the bubble size distribution, the assumption was made that bubble size distributions mirror the size distributions of interstitial pores. The values of the bubble/pore radius ratio that fit the model to data suggest that this assumption is inappropriate. Further research is required to develop an improved estimate of the bubble size distribution.

The experimental observations that were compared with the model were all backscatter measurements. The bistatic portion of the scattering model must be tested as soon as bistatic scattering data becomes available.

A MODEL FOR BISTATIC SCATTERING FROM TRAPPED GAS BUBBLES IN SANDY SEDIMENTS

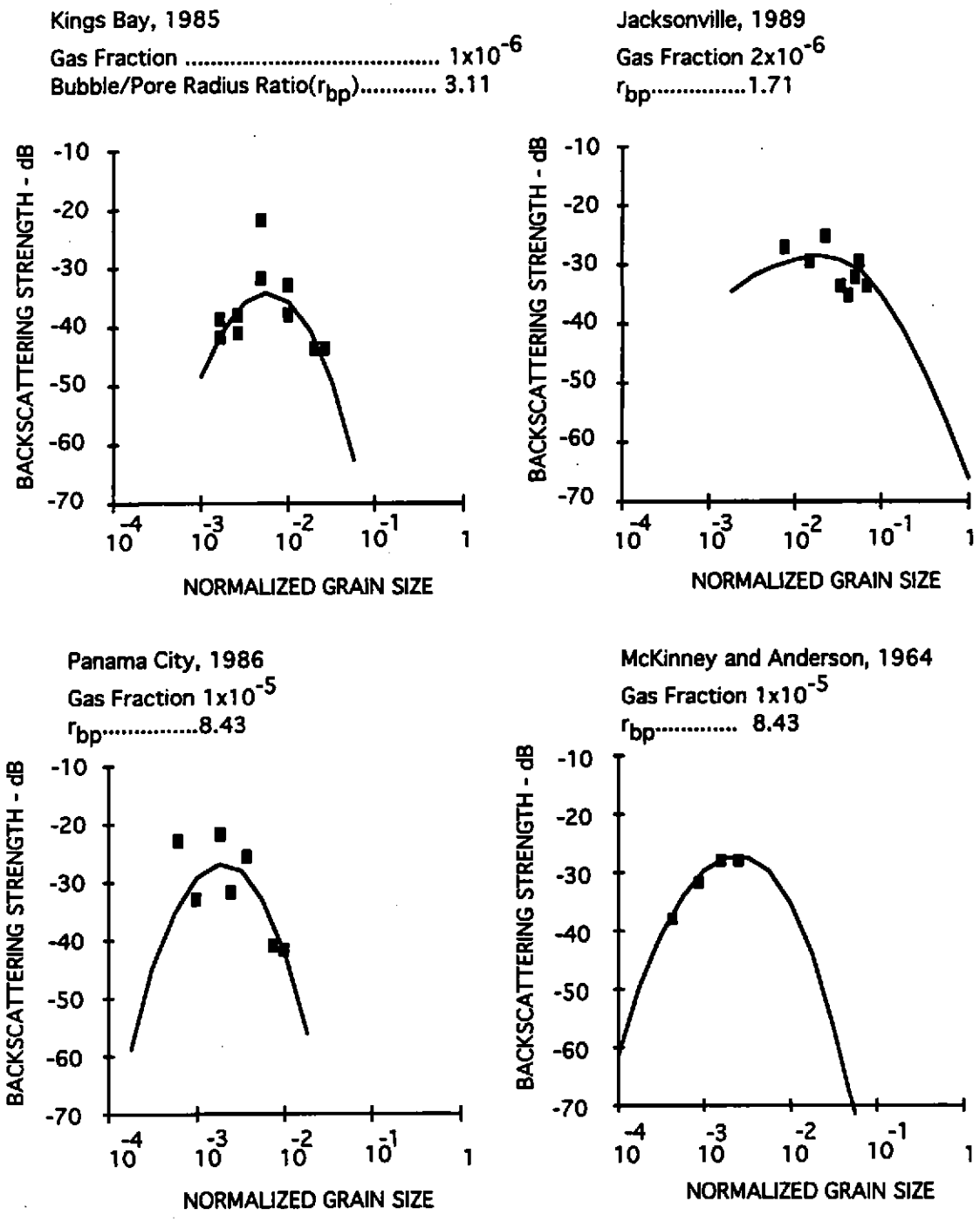

Figure 8. Comparison of experimental data with backscattering strengths predicted by Eq. (22).

A MODEL FOR BISTATIC SCATTERING FROM TRAPPED GAS BUBBLES IN SANDY SEDIMENTS

Table 1: Model parameters corresponding to the sediment sites of Fig. 8

Site		Kings Bay 1985	Panama City 1986	Jacksonville 1989	McKinney et.al. 1964
Fluid Density	(kg/m^3)	1000	1000	1000	1000
Fluid Bulk Modulus	(Pa)	$2.25x10^9$	$2.25x10^9$	$2.25x10^9$	$2.25x10^9$
Porosity		0.36	0.39	0.38	0.4
Grain Density	(kg/m^3)	2650	2650	2650	2650
Mean Grain Diameter	(ϕ)	1.30	2.51	0.84	3.0
Standard Deviation	(ϕ)	0.86	0.79	1.6	1.0
Pore Size Parameter	(m)	$1.09x10^{-4}$	$5.08x10^{-5}$	$3.89x10^{-4}$	$4.49x10^{-5}$
Viscosity	(kg/m-s)	$1.0x10^{-3}$	$1.0x10^{-3}$	$1.0x10^{-3}$	$1.0x10^{-3}$
Permeability	(m^2)	$2.15x10^{-10}$	$5.03x10^{-11}$	$2.87x10^{-9}$	$4.03x10^{-11}$
Virtual Mass Parameter		1.889	1.782	1.818	1.75
Grain Bulk Modulus	(Pa)	$7.0x10^9$	$7.0x10^9$	$7.0x10^9$	$7.0x10^9$
Frame Shear Modulus	(Pa)	$2.61x10^7$	$2.61x10^7$	$2.61x10^7$	$2.61x10^7$
Shear Log Decrement		0.15	0.15	0.15	0.15
Frame Bulk Modulus	(Pa)	$5.3x10^9$	$5.3x10^9$	$5.3x10^9$	$5.3x10^9$
Bulk Log Decrement		0.15	0.15	0.15	0.15
Gas Bulk Modulus	(Pa)	$2.48x10^5$	$2.48x10^5$	$2.48x10^5$	$2.48x10^5$
Gas Density	(Kg/m^3)	1.22	1.22	1.22	1.22
Gas Heat Conductivity	(cal/m-s-°c)	$5.6x10^{-3}$	$5.6x10^{-3}$	$5.6x10^{-3}$	$5.6x10^{-3}$
Gas Spec. Heat (Const Press)	(cal/Kg)	240	240	240	240
Gas Specific Heat Ratio, C_p/C_v		1.4	1.4	1.4	1.4
Bubble Surface Tension	(N/m^2)	0.075	0.075	0.075	0.075
Bubble/Pore Radius Ratio		3.11	8.43	1.71	8.43
Gas Content		$1.0x10^{-6}$	$1.0x10^{-5}$	$2.0x10^{-6}$	$1.0x10^{-5}$

A MODEL FOR BISTATIC SCATTERING FROM TRAPPED GAS BUBBLES IN SANDY SEDIMENTS

REFERENCES

[1] R E PATTERSON, 'Backscatter of sound from a rough boundary', J. Acoust. Soc. Am. **35**, 2010-2013 (1963).

[2] C S CLAY & H MEDWIN, *Acoustical Oceanography: Principles and Applications* (Wiley-Interscience, New York, 1977).

[3] A W NOLLE, W A HOYER, J F MIFSUD, W R RUNYAN, & M B WARD, 'Acoustic properties of water-filled sands', J. Acoust. Soc. Am. **35**, 1394 (1963).

[4] J H STOCKHAUSEN, 'Scattering from the volume of an inhomogeneous half-space', Naval Research Establishment (Dartmouth, N.S.) Report No. 63/9 (1963).

[5] A N IVAKIN & YU P LYSANOV, 'Underwater sound scattering by volume inhomogeneities of a bottom medium bounded by a rough surface', Sov. Phys. Acoust. **27**, 212-215 (1981).

[6] D R JACKSON, D P WINEBRENNER, & A.ISHIMARU, 'Application of the composite roughness model to high-frequency bottom backscattering', J. Acoust. Soc. Am. **79**, 1410-1422 (1986).

[7] N P CHOTIROS & F.A BOYLE, 'Gas bubbles in ocean sediments and high-frequency acoustic backscattering strength', presented at 121st Meeting of the Acoustical Society of America: J. Acoust. Soc. Am. **89**(4), Pt. 2, 1852 (1991).

[8] Ibid, Nolle etal.

[9] N P CHOTIROS & M L RAMAKER, 'High frequency acoustic penetration of sandy ocean sediments', presented at 121st Meeting of the Acoustical Society of America: J. Acoust. Soc. Am. **89**(4), Pt. 2, 1908 (1991).

[10] F A BOYLE & N P CHOTIROS, 'Experimental detection of a slow acoustic wave in sediment at shallow grazing angles', J. Acoust. Soc. Am. **91**, 2615-2619 (1992).

[11] M A BIOT, 'Theory of propagation of elastic waves in a fluid saturated porous solid. I low frequency range', J. Acoust. Soc. Am. **28**, 168-178 (1956).

[12] M A BIOT, 'Theory of propagation of elastic waves in a fluid saturated porous solid. II higher frequency range', J. Acoust. Soc. Am **28**, 179-191 (1956).

[13] M STERN, A BEDFORD, & H R MILLWATER, 'Wave reflection from a sediment layer with depth-dependent properties', J. Acoust. Soc. Am. **77**, 1781-1788 (1985)

[14] F A BOYLE & N P CHOTIROS, 'A model for high frequency acoustic backscatter from gas bubbles in sandy sediments at shallow grazing angles', submitted to J. Acoust. Soc. Am. for publication

[15] G S CARGILL, 'Radial distribution functions and microgeometry of dense random packings of hard spheres', in: *Physics and Chemistry of Porous Media*, D L Johnson and P N Sen, editors (American Institute of Physics, New York, 1984).

A MODEL FOR BISTATIC SCATTERING FROM TRAPPED GAS BUBBLES IN SANDY SEDIMENTS

[16] J L FINNEY & J WALLACE, J. Non-Cryst. Solids **34**, 165 (1981).

[17] R WILDT, ed., 'Acoustic Theory of Bubbles', in *Physics of Sound in the Sea*, N.D.R.C. Summary Technical Report Div. 6, (Washington, D.C., 1946),.Chap.28, Vol. 8.

[18] H MEDWIN, 'Acoustical Determinations of Bubble Size Spectra', J. Acoust. Soc. Am. **62**,1041-1044 (1977).

[19] J I DUNLOP, 'Propagation of acoustic waves in marine sediments, a review,' Exploration Geophysics **19**, 513-535 (1988).